Disorder and broad-angle iridescence from *Morpho*-inspired structures

Bokwang Song,[1] Seok Chan Eom,[1] and Jung H. Shin[2,1,*]

[1]*Dept. of Physics, KAIST, 335 Gwahangno, Yuseong-Gu, Daejeon 305-701, South Korea*
[2]*Graduate School of Nanoscience and Technology, KAIST, 335 Gwahangno, Yuseong-Gu, Daejeon, 305-701, South Korea*
[*]*jhs@kaist.ac.kr*

Abstract: The ordered, lamellae-structured ridges on the wing scales of *Morpho* butterflies give rise to their striking blue iridescence by multilayer interference and grating diffraction. At the same time, the random offsets among the ridges broaden the directional multilayer reflection peaks and the grating diffraction peaks that the color appears the same at various viewing angles, contrary to the very definition of iridescence. While the overall process is well understood, there has been little investigation into confirming the roles of each factor due to the difficulty of controllably reproducing such complex structures. Here we use a combination of self-assembly, selective etching, and directional deposition to fabricate *Morpho*-inspired structure with controlled random offsets. We find that while random offsets are necessary, it alone is not sufficient to produce the broad-angle reflection of *Morpho* butterflies. We identify diffraction as a critical factor for the bright, anisotropic broadening of the reflection peak of *Morpho* butterflies to a solid angle of 0.23 sr, and suggest random macroscopic surface curvature as a practical alternative, with an isotropic broad reflection peak whose solid angle can reach 0.11 sr at an incident angle of 60 ^{o}.

OCIS codes: (350.4238) Nanophotonics and photonic crystals; (310.6628) Subwavelength structures, nanostructures; (220.4241) Nanostructure fabrication; (050.1755) Computational electromagnetic methods; (330.0330) Vision, color, and visual optics.

References and links

1. P. Vukusic and J. R. Sambles, "Photonic structures in biology," Nature **424**(6950), 852–855 (2003).
2. M. Srinivasarao, "Nano-optics in the biological world: beetles, butterflies, birds, and moths," Chem. Rev. **99**(7), 1935–1962 (1999).
3. L. P. Biró and J. P. Vigneron, "Photonic nanoarchitectures in butterflies and beetles: valuable sources for bioinspiration," Laser Photon. Rev. **5**(1), 27–51 (2011).
4. S. Kinoshita, S. Yoshioka, and J. Miyazaki, "Physics of structural colors," Rep. Prog. Phys. **71**(7), 076401 (2008).
5. V. Sharma, M. Crne, J. O. Park, and M. Srinivasarao, "Structural origin of circularly polarized iridescence in jeweled beetles," Science **325**(5939), 449–451 (2009).
6. P. B. Clapham and M. C. Hutley, "Reduction of lens reflexion by moth eye principle," Nature **244**(5414), 281–282 (1973).
7. E. Iwase, K. Matsumoto, and I. Shimoyama, "The structural-color based on the mechanism butterfly wing coloring for wide viewing angle reflective display," in *Proceedings of 17th IEEE international conference on MEMS* (Maastricht Exhibition and Convention Centre, Maastricht, 2004), pp. 105–108.
8. R. A. Potyrailo, H. Ghiradella, A. Vertiatchikh, K. Dovidenko, J. R. Cournoyer, and E. Olson, "Morpho butterfly wing scales demonstrate highly selective vapour response," Nat. Photon. **1**(2), 123–128 (2007).
9. A. D. Pris, Y. Utturkar, C. Surman, W. G. Morris, A. Vert, S. Zalyubovskiy, T. Deng, H. T. Ghiradella, and R. A. Potyrailo, "Towards high-speed imaging of infrared photons with bio-inspired nanoarchitectures," Nat. Photon. **6**(3), 195–200 (2012).
10. K. Forberich, G. Dennler, M. C. Scharber, K. Hingerl, T. Fromherz, and C. J. Brabec, "Performance improvement of organic solar cells with moth eye anti-reflection coating," Thin Solid Films **516**(20), 7167–7170 (2008).

#212686 - $15.00 USD Received 23 May 2014; revised 21 Jul 2014; accepted 25 Jul 2014; published 4 Aug 2014

11. S. M. Doucet and M. G. Meadows, "Iridescence: a functional perspective," J. R. Soc. Interface **6**(Suppl 2), S115–S132 (2009).
12. S. Berthier, *Iridescences: The Physical Colors of Insects* (Springer, 2007).
13. C. W. Mason, "Structural colors in insects. I," J. Phys. Chem. **30**(3), 383–395 (1926).
14. C. W. Mason, "Structural colors in insects. II," J. Phys. Chem. **31**(3), 321–354 (1927).
15. C. W. Mason, "Structural colors in insects. III," J. Phys. Chem. **31**(12), 1856–1872 (1927).
16. S. Kinoshita and S. Yoshioka, "Structural colors in nature: the role of regularity and irregularity in the structure," ChemPhysChem **6**(8), 1442–1459 (2005).
17. Y. Takeoka, "Angle-independent structural coloured amorphous arrays," J. Mater. Chem. **22**(44), 23299 (2012).
18. S. Berthier, *Photonique de Morphos* (Springer, 2010).
19. S. Kinoshita, S. Yoshioka, and K. Kawagoe, "Mechanisms of structural colour in the Morpho butterfly: cooperation of regularity and irregularity in an iridescent scale," Proc. Biol. Sci. **269**(1499), 1417–1421 (2002).
20. H. Ghiradella, "Light and color on the wing: structural colors in butterflies and moths," Appl. Opt. **30**(24), 3492–3500 (1991).
21. A. Saito, Y. Ishikawa, Y. Miyamura, M. Akai-Kasaya, and Y. Kuwahara, "Optimization of reproduced Morpho-blue coloration," Proc. SPIE **6767**, 676706 (2007).
22. S. Kinoshita, S. Yoshioka, Y. Fujii, and N. Okamoto, "Photophysics of structural color in the Morpho butterflies," Forma **17**, 103–121 (2002).
23. P. Vukusic, J. R. Sambles, C. R. Lawrence, and R. J. Wootton, "Quantified interference and diffraction in single Morpho butterfly scales," Proc. Biol. Sci. **266**(1427), 1403–1411 (1999).
24. A. Saito, M. Yonezawa, J. Murase, S. Juodkazis, V. Mizeikis, M. Akai-Kasaya, and Y. Kuwahara, "Numerical analysis on the optical role of nano-randomness on the Morpho butterfly's scale," J. Nanosci. Nanotechnology **11**(4), 2785–2792 (2011).
25. J. Boulenguez, S. Berthier, and F. Leroy, "Multiple scaled disorder in the photonic structure of Morpho rhetenor butterfly," Appl. Phys., A Mater. Sci. Process. **106**(4), 1005–1011 (2012).
26. D. Zhu, S. Kinoshita, D. Cai, and J. B. Cole, "Investigation of structural colors in Morpho butterflies using the nonstandard-finite-difference time-domain method: Effects of alternately stacked shelves and ridge density," Phys. Rev. E Stat. Nonlin. Soft Matter Phys. **80**(5), 051924 (2009).
27. M. Kambe, D. Zhu, and S. Kinoshita, "Origin of retroreflection from a wing of the Morpho butterfly," J. Phys. Soc. Jpn. **80**(5), 054801 (2011).
28. S. Yoshioka and S. Kinoshita, "Structural or pigmentary? Origin of the distinctive white stripe on the blue wing of a Morpho butterfly," Proc. Biol. Sci. **273**(1583), 129–134 (2006).
29. K. Watanabe, T. Hoshino, K. Kanda, Y. Haruyama, T. Kaito, and S. Matsui, "Optical measurement and fabrication from a Morpho-butterfly-scale quasistructure by focused ion beam chemical vapor deposition," J. Vac. Sci. Technol. B **23**(2), 570–574 (2005).
30. A. Saito, S. Yoshioka, and S. Kinoshita, "Reproduction of the Morpho butterfly's blue: arbitration of contradicting factors," Proc. SPIE **5526**, 188–194 (2004).
31. R. H. Siddique, S. Diewald, J. Leuthold, and H. Hölscher, "Theoretical and experimental analysis of the structural pattern responsible for the iridescence of Morpho butterflies," Opt. Express **21**(12), 14351–14361 (2013).
32. K. Chung, S. Yu, C. J. Heo, J. W. Shim, S. M. Yang, M. G. Han, H. S. Lee, Y. Jin, S. Y. Lee, N. Park, and J. H. Shin, "Flexible, angle-independent, structural color reflectors inspired by morpho butterfly wings," Adv. Mater. **24**(18), 2375–2379 (2012).
33. D. Ge, L. Yang, G. Wu, and S. Yang, "Spray coating of superhydrophobic and angle-independent coloured films," Chem. Commun. **50**(19), 2469–2472 (2014).
34. L. P. Biró, K. Kertész, E. Horváth, G. I. Márk, G. Molnár, Z. Vértesy, J.-F. Tsai, A. Kun, Zs. Bálint, and J. P. Vigneron, "Bioinspired artificial photonic nanoarchitecture using the elytron of the beetle Trigonophorus rothschildi varians as a 'blueprint'," J. R. Soc. Interface **7**(47), 887–894 (2010).
35. I. Tamáska, Z. Vértesy, A. Deák, P. Petrik, K. Kertész, and L. P. Biró, "Optical properties of bioinspired disordered photonic nanoarchitectures," Nanopages **8**(2), 17–30 (2013).
36. K. Chung and J. H. Shin, "Range and stability of structural colors generated by Morpho-inspired color reflectors," J. Opt. Soc. Am. A **30**(5), 962–968 (2013).
37. J. B. Schneider, "Understanding the FDTD method" (2010), www.eecs.wsu.edu/~schneidj/ufdtd.
38. P. Pirih, B. D. Wilts, and D. G. Stavenga, "Spatial reflection patterns of iridescent wings of male pierid butterflies: curved scales reflect at a wider angle than flat scales," J. Comp. Physiol. A Neuroethol. Sens. Neural Behav. Physiol. **197**(10), 987–997 (2011).

1. Introduction

Many insects possess intricate structures in the wings and scales that cause diffraction, interference, scattering, and many combinations thereof [1–3]. They affect reflection [4], polarization [5], and absorption [6] of the incident light, and are responsible for some of the most impressive optical phenomena in the natural world. Studying these phenomena has led

#212686 - $15.00 USD Received 23 May 2014; revised 21 Jul 2014; accepted 25 Jul 2014; published 4 Aug 2014

to not only increased knowledge, but also possible breakthroughs in many diverse and critical applications such as displays [7], sensing [8,9], and energy conversions and solar cells [10].

One particular phenomenon that has attracted a great deal of attention is iridescence, the property of certain surfaces to display brilliant structural colors that change color with the viewing angle [11–15]. Some insects, however, show structural colors that appear the same over a broad range of viewing angles, contrary to the very definition of iridescence [16,17]. One well-known example of such broad-angle iridescence is the butterflies of genus *Morpho* from Central and South America [18]. They are well-known not only for their bright, blue iridescence, but also for the fact that their color seems to remain relatively stable over a wide range of viewing angles, contrary to the very definition of iridescence [19]. This seeming paradox has attracted a great deal of attention, and by now, the general principles have been well understood and investigated theoretically [19–28]: the blue color arises from interference within the multilayered ridges of chitin that cover the scales on the wings [20]; the dense packing of the narrow, discrete ridges lead to high reflectivity, and also gives rise to additional effect of diffraction [21–23]; and finally, the random offsets among the ridges removes the coherence, and broaden the sharp peaks associated with multilayer reflection and diffraction such that the color appears relatively stable across wide viewing angles [19, 24–26]. In addition, there are contributions from layer-offset within ridges, absorption, and scattering as well [26–28]. On the other hand, verifying these principles in a controlled manner using a man-made structure has been less successful due to the complexities required. Thus, previous experiments such as direct nano-fabrication of individual multilayer structures [29], use of binary height offsets [30] or two-dimensional structures [31] have proved the overall validity of the principles, but did not provide a quantitative analysis of their effect on the bright, broad-angle blue of *Morpho* butterflies.

Recently, we have demonstrated that by spin-coating a close-packed monolayer of randomly sized silica microspheres, a substrate with random offsets can be generated and used to fabricate *Morpho*-inspired structural reflectors that show bright, angle-independent color [32]. This approach differed from other, recent reports on successfully introducing randomness for broad-angle iridescence [33] in that the color was controlled by multilayer reflection as in actual *Morpho* butterflies, thus enabling accurate color tuning across a wide range, and that a continuous distribution of disorder, both vertical and horizontal, was generated spontaneously in a large area without any lithography or etching [34,35]. Unfortunately, the use of close-packed spheres creates identical horizontal and vertical offsets such that one cannot control the vertical offsets independently, and suppresses the effect of diffraction due to the continuous multilayer structure. In this paper, we use the silica microspheres as selective etch mask to fabricate a substrate with controlled vertical disorder in order to investigate its effect on the broadening of the reflection peaks. Based on quantitative comparison with actual *Morpho* butterflies and numerical simulations, we find that while vertical disorder is necessary to broaden the reflection peaks, it alone is not sufficient. In order to fully replicate the bright, broad-angle blue of *Morpho* butterflies, it is critical to include other effects such as diffraction that suppress the specular reflection and provide non-specular reflection. Surprisingly, we find that random macroscopic surface curvature, which is often overlooked in theoretical analysis, can be quite effective in generating such bright, broad-angle reflection.

#212686 - $15.00 USD Received 23 May 2014; revised 21 Jul 2014; accepted 25 Jul 2014; published 4 Aug 2014

2. Fabrication with disorder control

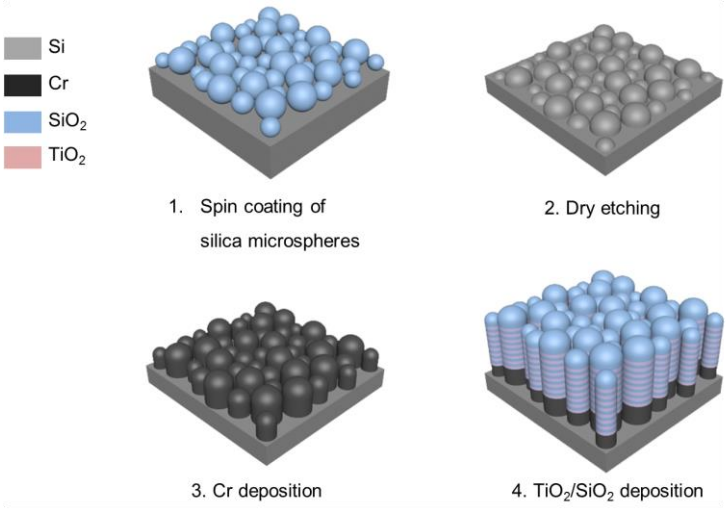

Fig. 1. A schematic description of the fabrication process.

A monolayer of silica microspheres with diameters ranging from 250 nm to 440 nm (ethanolic silica suspension with 8 wt%) was spin-coated (3000 rpm) on a Si wafer, and then fixed to the Si substrate by a high temperature (1000 °C) annealing with oxygen gas. The microspheres were then used as etch-mask during CHF_3/O_2 plasma etching to transfer the texture of the randomly sized spheres onto the underlying Si substrate. By controlling the gas flow (CHF_3: 30 sccm, O_2: 0 sccm to 10 sccm) and operating pressure (15 mT to 40 mT), we could selectively etch either Si or SiO_2, either to enhance or to diminish the original height difference among the silica microspheres. Afterward, a 300 nm thick layer of Cr was deposited to serve as the absorption layer for higher color purity [32], similar to melanin-containing scales in *Morpho* butterflies [28]. Finally, 8 pairs SiO_2/TiO_2 layers of 73 nm and 38 nm, respectively, were sputter-deposited. The deposition pressure was kept intentionally low at 0.3 mT to induce directional growth and preservation of the random texture of the substrate in the deposited multilayers. A schematic description of the fabrication process is shown in Fig. 1.

Figure 2 shows the scanning-electron microscope (SEM) images of the original monolayer of silica microspheres and the etched Si substrates, and their vertical and horizontal offsets as measured by SEM and atomic force microscope (AFM). We see that using selective etching, the distribution of the vertical offsets can be controlled such that the standard deviation is reduced from 46 nm to 12 nm. On the other hand, the distribution of the horizontal offsets remains almost unchanged (Table 1), confirming that we are isolating the effect of the randomness in the vertical offsets.

#212686 - $15.00 USD Received 23 May 2014; revised 21 Jul 2014; accepted 25 Jul 2014; published 4 Aug 2014

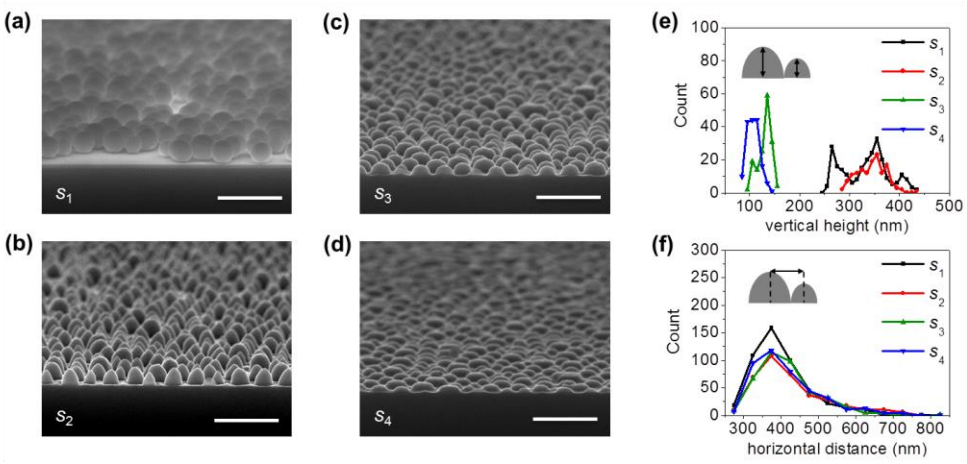

Fig. 2. Structural analysis of disorder-controlled substrate. Cross-section SEM image (10 °-tilted) of (a) monolayer of randomly sized silica microspheres on the Si substrate (substrate s_1), (b) etched Si substrate with SiO_2/Si etching selectivity of 1 (substrate s_2), (c) with etching selectivity 2 (substrate s_3), and (d) with etching selectivity 3 (substrate s_4). (e) Vertical height distribution of the substrates s_1 - s_4, as measured by SEM and AFM. The black arrows in inset indicate vertical height measured. (f) The horizontal distance distribution of the substrates s_1 - s_4 as measured by SEM and AFM. The black arrow in inset indicates horizontal distance measured. Scale bars, 1μm.

Table 1. The statistical values of nanoscale offsets of the substrates in Fig. 2.

	Vertical height		Horizontal distance	
substrate	Mean value	Standard deviation	Mean value	Standard deviation
s_1	333	46	399	76
s_2	343	28	428	87
s_3	130	14	416	80
s_4	106	12	414	86

Unit: nm

3. Optical analysis

3.1. Reflectance measurement methods

Angular and normal reflectance were measured for optical analysis. Angular reflectance was measured using a goniospectrophotometer consisting of two optical fibers [Fig. 3]. The incident light from deuterium-halogen source (Avantes, AvaLight-DH-S-BAL) was guided and illuminated by an optical fiber, and collimated by lens. The diameter of beam spot on the samples was 5 mm. Reflected beam was coupled into the other optical fiber and measured by a spectrometer (Avantes, AvaSpec-2048). Al mirror was used for the reference. Measured data was calibrated by theoretical reflectance value of Al mirror. Normal reflectance was measured using a reflection probe separated into 2 connectors (Avantes, FCR-7UV200-2-ME). A light source was connected with one of the two connectors and illuminated through the probe end. Reflected beam was coupled into the probe end and measured by a spectrometer connected with the other connector. The same light source, spectrometer, and reference as angular reflectance measurements were used for normal reflectance measurements. In case of *Morpho* butterflies, the plane of incidence was adjusted to be parallel to the multilayered ridges. A schematic description of the measurement setup is shown in Fig. 3.

#212686 - $15.00 USD Received 23 May 2014; revised 21 Jul 2014; accepted 25 Jul 2014; published 4 Aug 2014

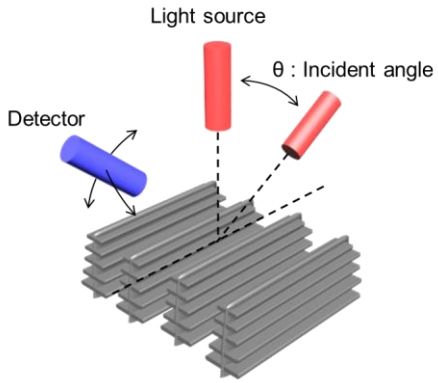

Fig. 3. A schematic view of measurement setup for angular reflectance.

3.2. Results and analysis

Figure 4 shows the SEM and optical images of the *Morpho* butterflies and deposited multilayer films, normal reflectance spectra normalized to max value, and the corresponding colors. Note that the multilayer thin films deposited on both silica microspheres and etched Si substrates show the random undulations. However, both the continuous nature of the multilayers, as well as their smaller degree of undulations, are different from the discrete, 3D photonic-crystal like ridge structure of *Morpho* butterflies. Part of the reason for such differences in size is the higher refractive index of the deposited thin film. However, while the physics of reflection from such disordered multilayer structures are the same, these differences in structural details can lead to significant differences in their optical properties, as shall be discussed in detail below. The optical images were taken under ambient light conditions, and the reflectance spectra were measured using a conventional spectrometer under normal directional light conditions. For comparison, we also show the results from a wrinkled multilayer film formed by depositing on a monolayer of random-sized silica microspheres unfixed to the Si substrate, as discussed in [32], K. Chung et al., and from *Morpho rhetenor* and *Morpho didius* butterflies. We find that the normal reflectance spectra, and the corresponding color, of the deposited films are very similar to each other, regardless of the vertical disorder or flatness of the film, confirming that the periodicity of multilayers is the dominant factor in determining the color [36]. However, the optical images clearly show the difference in appearance. While the wrinkled film appears shiny and bright like *Morpho* butterflies, the flat films appear quite dark, becoming darker as vertical disorder is decreased.

#212686 - $15.00 USD Received 23 May 2014; revised 21 Jul 2014; accepted 25 Jul 2014; published 4 Aug 2014

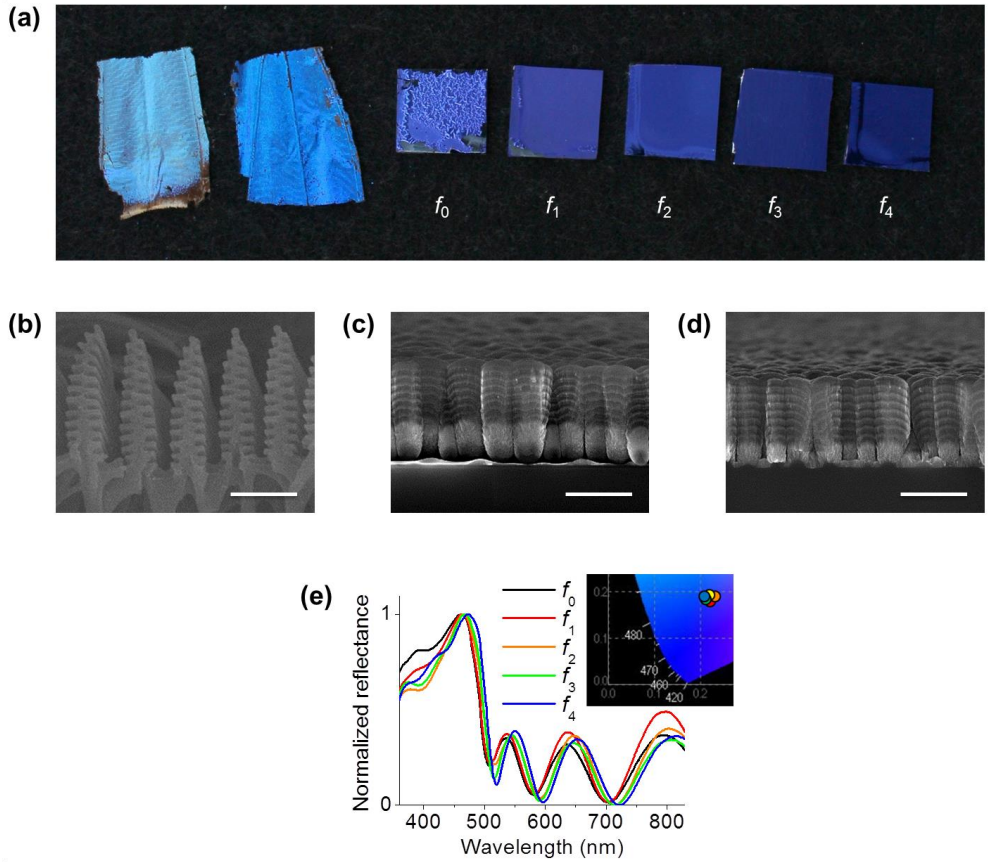

Fig. 4. Images and normal reflectance. (a) Optical images of the wing of *Morpho didius*, the wing of *Morpho rhetenor*, a wrinkled multilayer film deposited on s_1 unfixed to the Si substrate (defined as f_0), a flat multilayer film deposited on s_1 fixed to the Si substrate (defined as f_1), flat multilayer films deposited on s_2 - s_4 (defined as f_2 - f_4) from left to right. (b) Cross-sectional SEM image of multilayered ridges on the scale of *Morpho rhetenor* butterfly. (c) Cross-sectional SEM image of the deposited multilayer films on microspheres. (d) Cross-sectional SEM image of the deposited multilayer films on the etched Si substrate f_3. (e) Normal reflectance spectra, normalized to the max value, of the deposited multilayer films f_0 - f_4. Inset: Corresponding color coordinates on the 1931 CIE diagram. Scale bars, 1μm.

The reason for the difference in appearance can be found in Figs. 5, 6, 7, and 8 that shows the angular distribution of reflectance at different incident angles, measured at 460nm wavelength, the peak wavelength of the films [Fig. 4(e)] and *Morpho* butterflies as reported by [22], S. Kinoshita et al. We find that the reflections from flat films are all dominated by specular reflection peaks. Still, as Figs. 8(d)–8(f) show, increasing the vertical disorder drastically reduces the specular reflection intensity from 72% to 10% with concomitant broadening of the reflection peak, consistent with previous results [32]. Such effect of disorder is consistent with a similar observation has been reported before [35], albeit with a smaller set of samples and variations in disorder. However, such broadening pales in comparison to that observed from *Morpho* butterflies whose reflection peak, as shown in Fig. 5, is very broadly spread out, with no discernible specular reflection peak. Note, however, that the broadening of the reflection peak from *Morpho* butterflies is highly anisotropic, being spread out in a circular arc perpendicular to the plane of incidence. The solid angle extended

#212686 - $15.00 USD Received 23 May 2014; revised 21 Jul 2014; accepted 25 Jul 2014; published 4 Aug 2014

by the reflection peak, as measured from full width half maximum, can be as large as 0.23 sr, as observed from *Morpho rhetenor* butterfly at an incidence angle of 30 °.

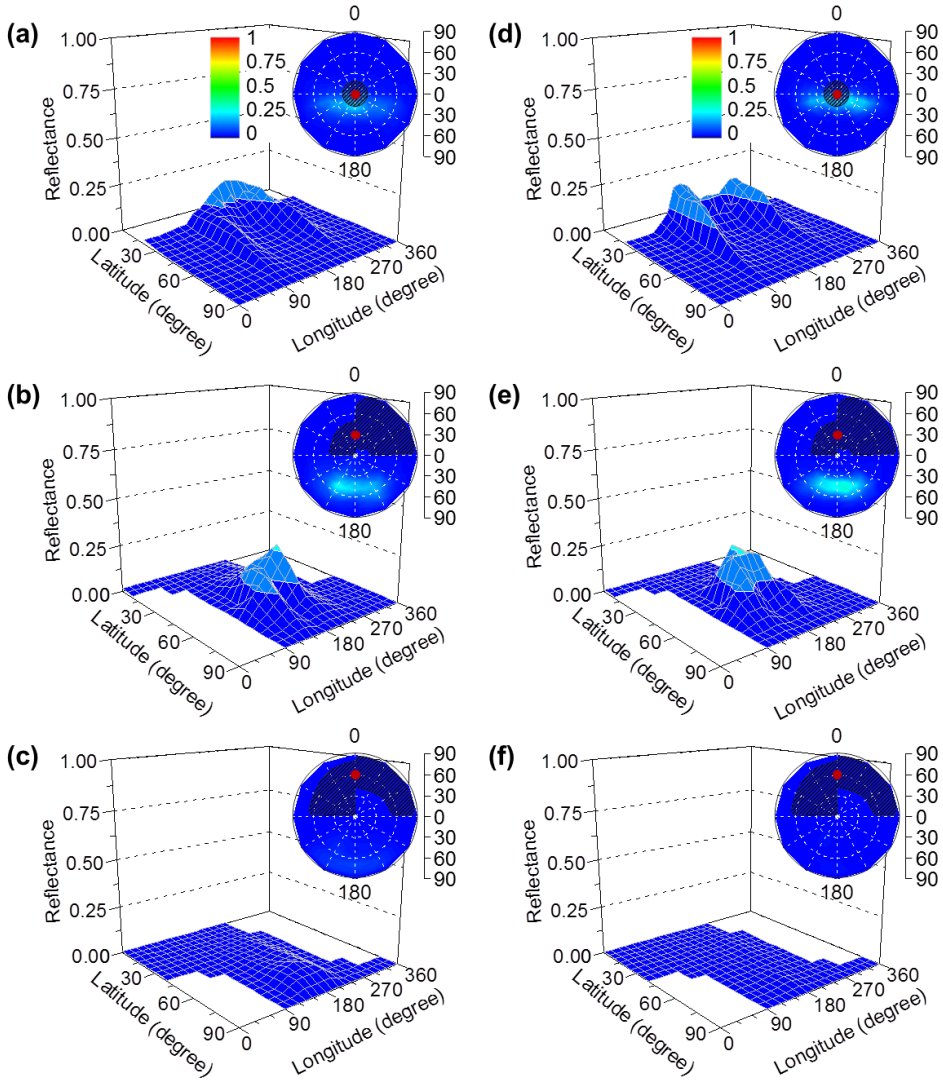

Fig. 5. Angular reflectance. (a-c) Angular distribution of reflectance of *Morpho didius* at incident angle of 0 ° (a), 30 ° (b), 60 ° (c) measured at wavelength of 460 nm. The ridges of *Morpho* butterflies were set to be parallel to the plane of incidence as seen in Fig. 3. Inset: two-dimensional polar plot. Red dots indicate the source positions. Shaded regions indicate regions where no data could be collected due to limitations of the measurement setup limit. (d-f) Corresponding data for *Morpho rhetenor*.

#212686 - $15.00 USD Received 23 May 2014; revised 21 Jul 2014; accepted 25 Jul 2014; published 4 Aug 2014

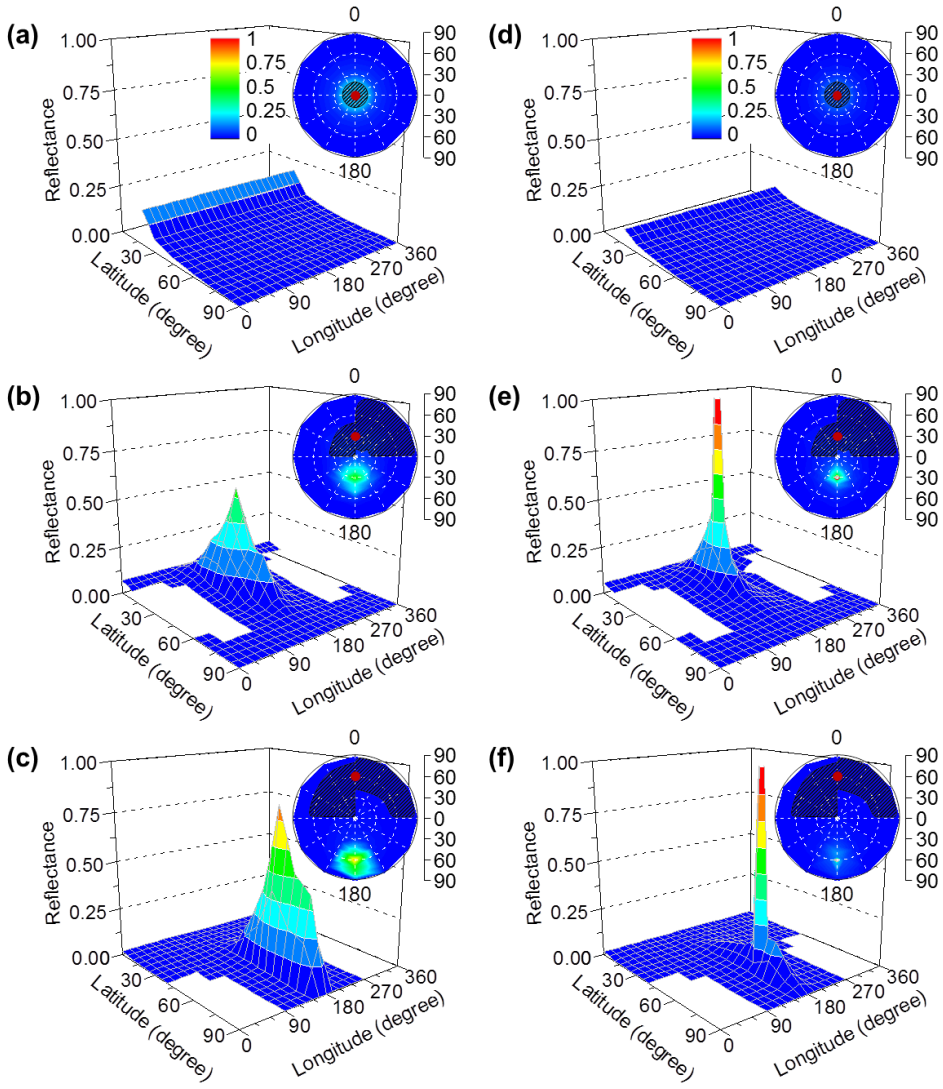

Fig. 6. Angular reflectance. (a-c) Angular distribution of reflectance of f_0 at incident angle of 0 ° (a), 30 ° (b), 60 ° (c) measured at wavelength of 460 nm. Inset: two-dimensional polar plot. Red dots indicate the source positions. Shaded regions indicate regions where no data could be collected due to limitations of the measurement setup limit. (d-f) Corresponding data for f_1.

#212686 - $15.00 USD Received 23 May 2014; revised 21 Jul 2014; accepted 25 Jul 2014; published 4 Aug 2014

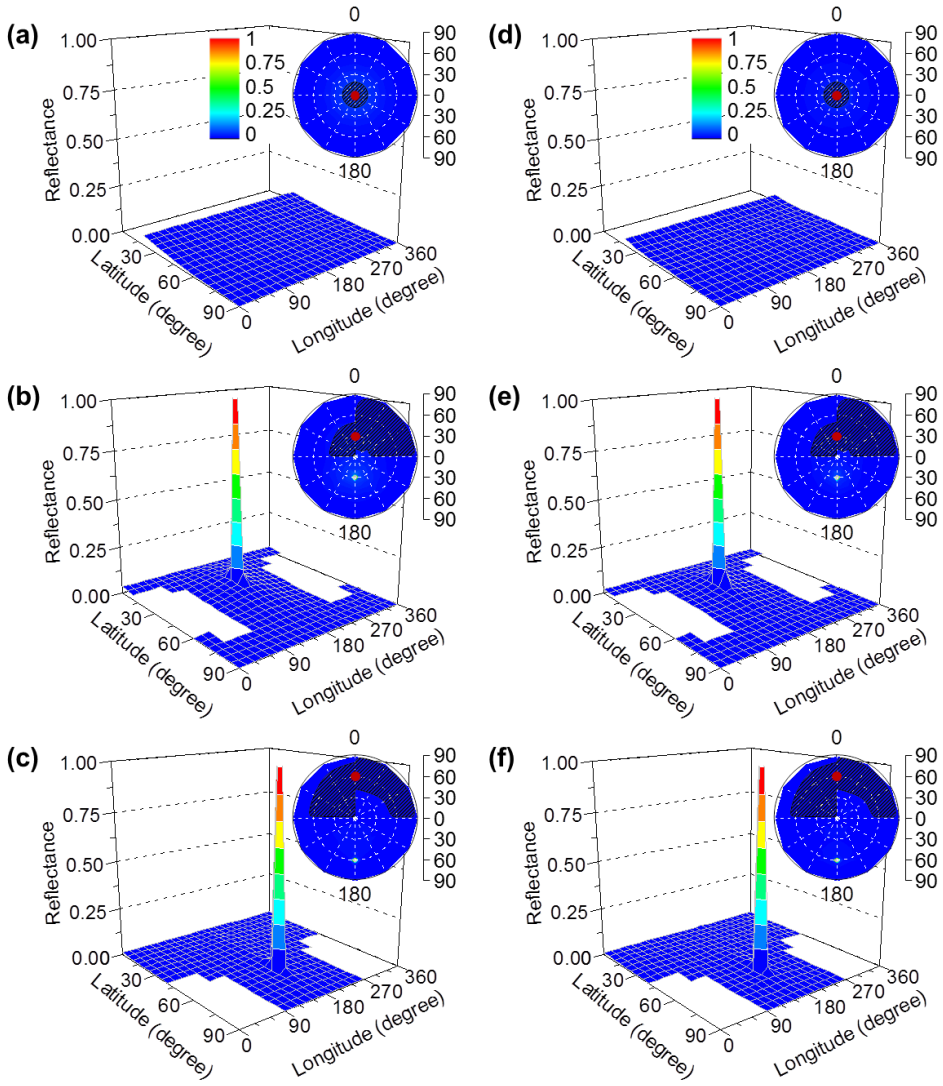

Fig. 7. Angular reflectance. (a-c) Angular distribution of reflectance of f_2 at incident angle of 0 ° (a), 30 ° (b), 60 ° (c) measured at wavelength of 460 nm. Inset: two-dimensional polar plot. Red dots indicate the source positions. Shaded regions indicate regions where no data could be collected due to limitations of the measurement setup limit. (d-f) Corresponding data for f_3.

#212686 - $15.00 USD Received 23 May 2014; revised 21 Jul 2014; accepted 25 Jul 2014; published 4 Aug 2014

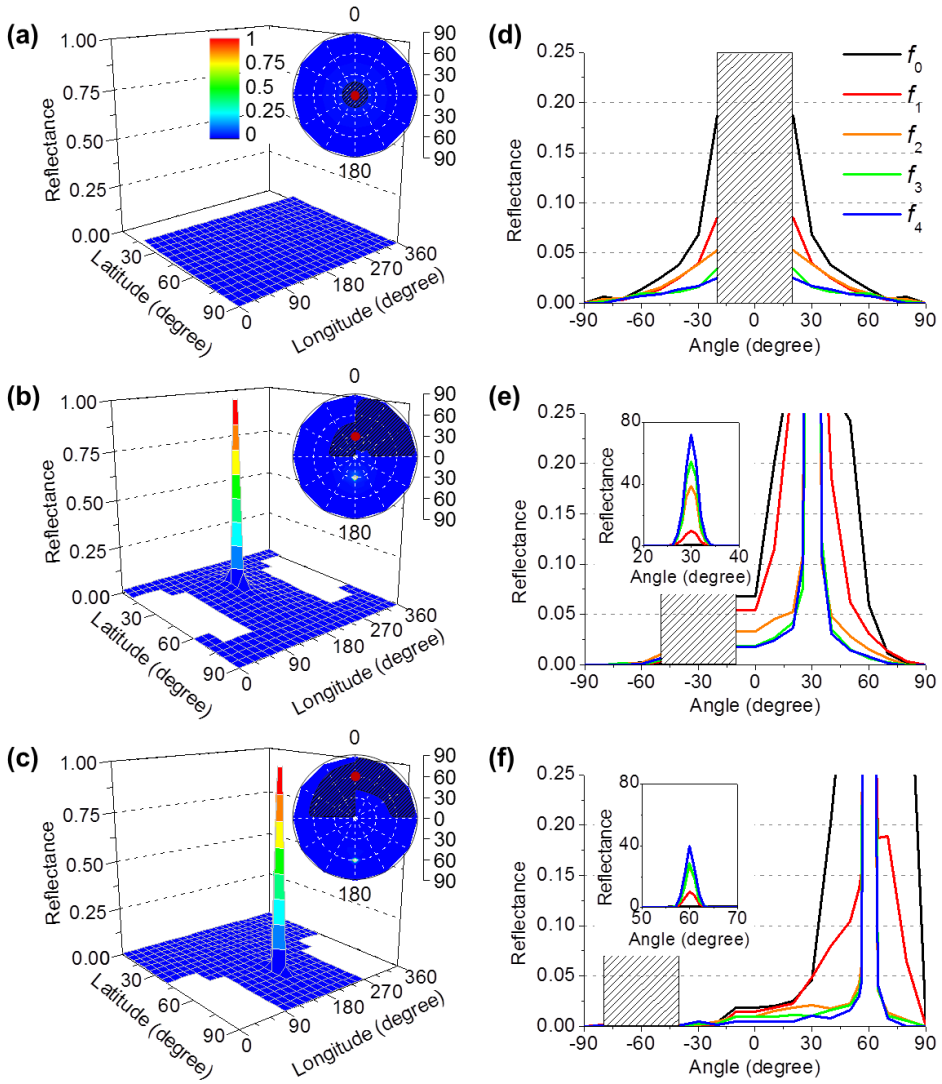

Fig. 8. Angular reflectance. (a-c) Angular distribution of reflectance of f_4 at incident angle of 0 ° (a), 30 ° (b), 60 ° (c) measured at wavelength of 460 nm. Inset: two-dimensional polar plot. Red dots indicate the source positions. Shaded regions indicate regions where no data could be collected due to limitations of the measurement setup limit. (d-f) Angular distribution of reflectance of f_0 - f_4 on the plane of incidence at incident angle of 0 ° (d), 30 ° (e), 60 ° (f). Inset: Plot with larger scale. All reflectance data were measured at 460nm wavelength.

Such differences demonstrate that other mechanisms in addition to random vertical offsets are necessary to fully generate the broad-angle reflection characteristic of *Morpho* butterflies. One such mechanism is large-angle diffraction from the ridge array [21]. While diffraction from periodic structures normally leads to sharp diffraction peaks, previous investigations have suggested that random offsets blur such sharp diffraction peaks, leading to continuous, broad-angle reflection as shown in Fig. 5 [19, 24–26]. We confirm such cooperation between diffraction and random offsets by numerical simulations. Using a structure shown schematically in Fig. 9, reflected intensities have been calculated using two dimensional finite element method with perfectly matched layer (PML) boundary conditions. An unpolarized monochromatic plane wave was used for incident light. Calculated wavelengths are from 380

#212686 - $15.00 USD Received 23 May 2014; revised 21 Jul 2014; accepted 25 Jul 2014; published 4 Aug 2014

nm to 580 nm with 40 nm interval. Structure size was nearly 1 × 10 μm, which contains about 30 reflective elements as seen in the Fig. 9. Each element is composed of 8 pairs SiO_2/TiO_2 layer with experimentally determined material parameters. A Cr layer and silica microsphere were omitted since the transmitted light could be absorbed by PML under the structure. All results show far-field reflected intensities that were obtained by near-to-far-field transformation [37] of calculated scattered near-field above 1 μm from the structure. In all cases, results from 5 statistically identical structures were averaged.

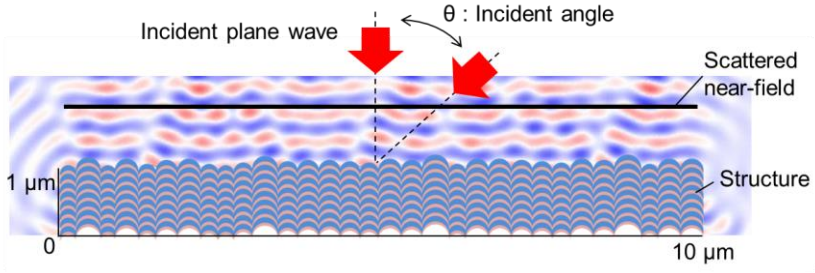

Fig. 9. A schematic view of simulation method.

The results of simulations are summarized in Fig. 10. From Figs. 10(a)–10(c), we confirm that introducing random vertical offsets to a continuous multilayer reduces the specular reflection peak, and introduces significant reflection at non-specular angles. However, as Figs. 10(d)–10(f) show, diffraction provides much larger non-specular reflection intensity at greater angles than random vertical offset alone can. Without random offsets, only sharp diffraction peaks are observed. When combined with vertical offsets, however, strong reduction of the specular reflection intensity to less than 20% and continuous non-specular reflection from −30° to + 30° similar to that observed from *Morpho* butterflies can be achieved.

It must be noted, however, that the sample f_o, which cannot cause any diffraction due to its continuous nature, and is identical to sample f_1 except for being wrinkled, has far lower specular reflection intensity than sample f_1, and a reflection peak whose width is comparable to that of *Morpho* butterflies. In fact, at highly oblique incidence angle of 60 °, the reflection peak from sample f_o with its wrinkled, continuous multilayer film is much higher than that from *Morpho* butterflies, and is broadened isotropically as well, with a solid angle that can be as large as 0.11 sr. This is consistent with, and may explain, previous reports that such *Morpho*-inspired thin films provide higher color stability against changing viewing angles [32], and suggests that diffraction is not essential for generating broad-angle reflections of *Morpho* butterflies. Instead, any mechanism such as random surface curvature that can provide strong non-specular reflections at large angles [38] may be used, as long as there also exists random vertical offset to blur and broaden the reflection peaks. Indeed, it is interesting to note that the sample f_o, whose wrinkles are of the size of several hundred μm [32], has a similar extent of disorder, ranging from tens of nm to several hundred μm, as *Morpho* butterfly [25].

#212686 - $15.00 USD Received 23 May 2014; revised 21 Jul 2014; accepted 25 Jul 2014; published 4 Aug 2014

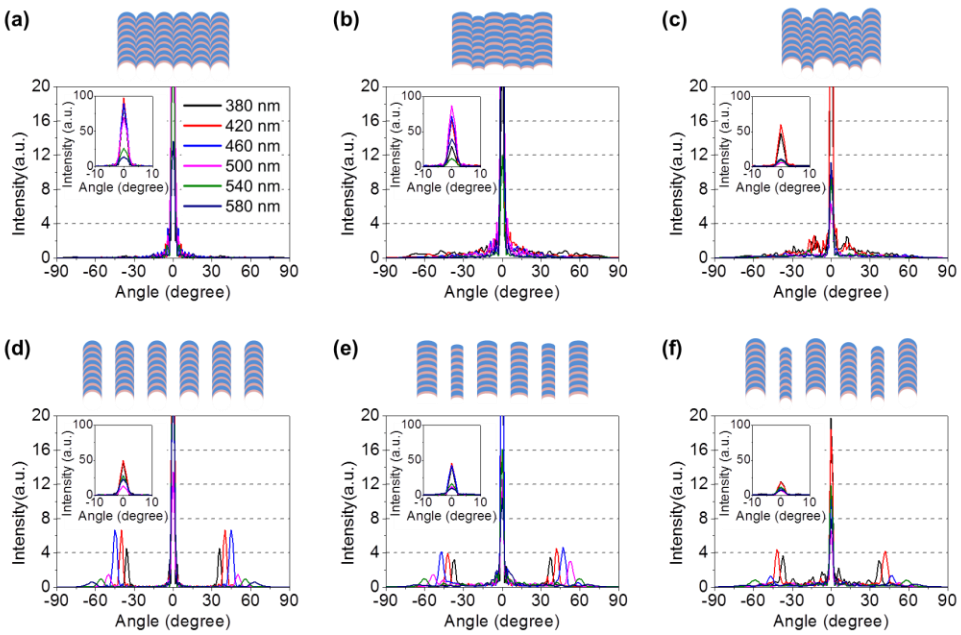

Fig. 10. Calculated far-field reflection intensities of (a) continuous multilayer structures deposited on a layer of uniformly sized microspheres of diameter 350 nm; (b) continuous multilayer structure with half of the random offsets of sample f_1 in Fig. 4; (c) continuous multilayer with the same random offsets as sample f_1 in Fig. 4. (d-f) Calculated far-field reflection intensities of structures designed by applying 300 nm gap spacing to the structures in (a)-(c). Schematic views of structure are on top. All calculation were performed under normal incident light. Insets: Plot with larger scale.

Figure 11 shows the effects of changing the multilayer pairs, gap spacing, and the incident angle. We find that, as expected, increasing the multilayer pair increases the reflected intensity, while increasing the gap spacing and the incidence angle reduces the reflected intensity. However, the reflected intensity from films with random disorder show much weaker dependence on such parameters than that from uniform films, consistent with the large body of reports on the importance of disorder for stable iridescence. Still, the fact that varying these parameters changes the reflected intensity indicates that a careful optimization of all such parameters in addition to the degree of disorder is necessary for practical applications.

#212686 - $15.00 USD Received 23 May 2014; revised 21 Jul 2014; accepted 25 Jul 2014; published 4 Aug 2014

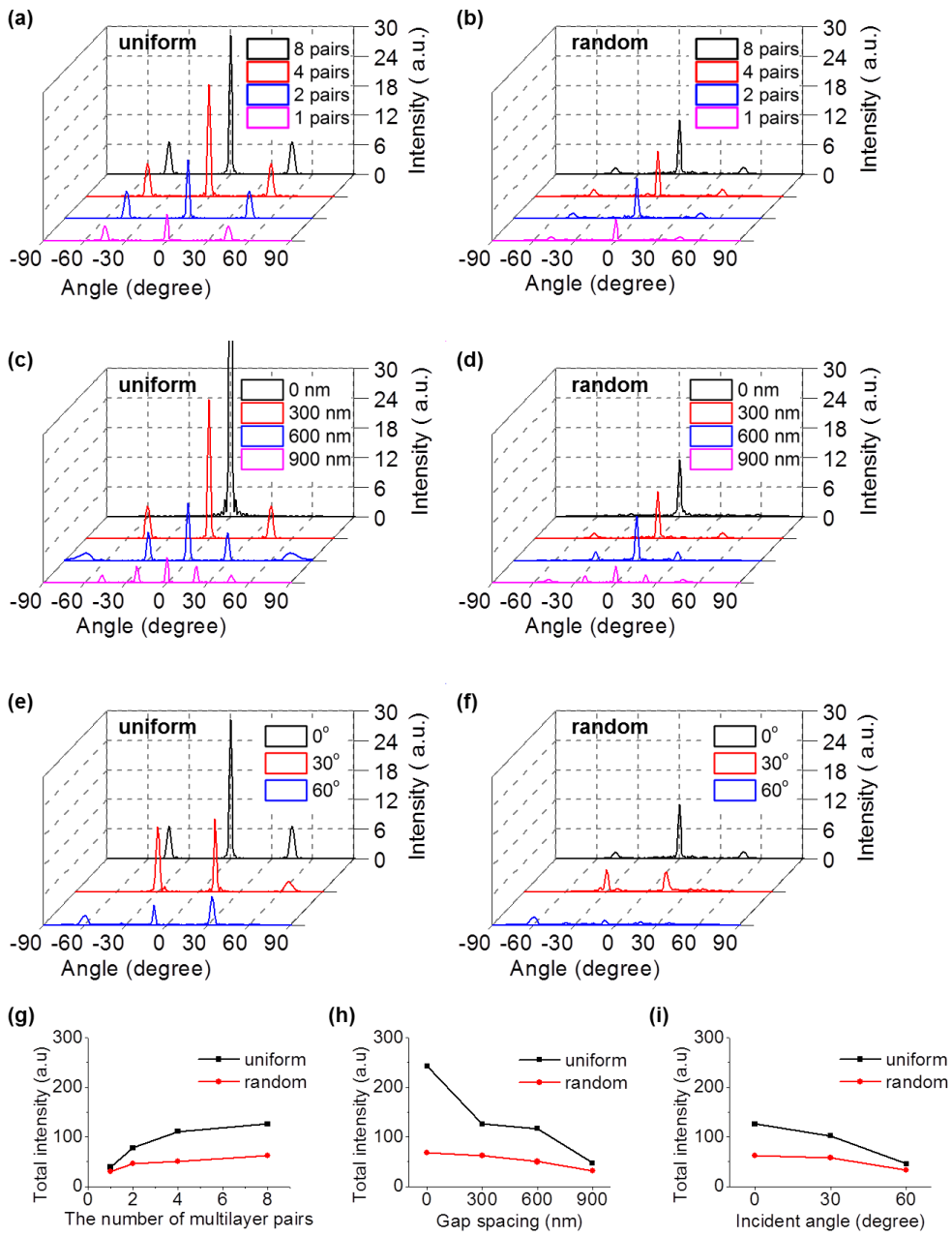

Fig. 11. The effect of structural parameter. Calculated far-field reflection intensities of 300 nm gap-applied uniform (the structure in Fig. 10(d)) and random (the structure in Fig. 10(f)) structure with changing (a-b) the number of multilayer pairs under normal incident light; (c-d) the gap spacing between the neighboring elements under normal incident light; (e-f) the incident angle, at wavelength of 460 nm. (g-i) The dependence of total far-field reflection intensities upon each parameter . All calculations were performed at 460nm wavelength.

5. Conclusion

In conclusion, we have investigated the effect of nanoscale disorder in *Morpho*-inspired structures. By directly controlling the vertical disorder in the multilayer structure, we show

#212686 - $15.00 USD Received 23 May 2014; revised 21 Jul 2014; accepted 25 Jul 2014; published 4 Aug 2014

that while vertical disorder is an essential ingredient in broadening the reflection peaks, it is not sufficient. In case of *Morpho* butterflies, diffraction plays a critical role to fully generate the broad reflection; however, other methods to suppress specular reflection and generate broad reflections such as random surface curvature can work just as well, as we demonstrate by bright, broad-angle reflection of wrinkled *Morpho*-inspired thin films.

Acknowledgments

This work was supported in part by the National Research Foundation of Korea (NRF) grant funded by the Korea government (MSIP) (Grant No. 2010-0029255, GRL: Grant No. K20815000003-11A0500-00310).

#212686 - $15.00 USD Received 23 May 2014; revised 21 Jul 2014; accepted 25 Jul 2014; published 4 Aug 2014